Food and Bioprocess Technology
https://doi.org/10.1007/s11947-018-2160-z

ORIGINAL PAPER

Bionanocomposite Films Prepared from Corn Starch With and Without Nanopackaged Jamaica (*Hibiscus sabdariffa*) Flower Extract

Luis A. Toro-Márquez[1,2] · Danila Merino[2] · Tomy J. Gutiérrez[2]

Received: 24 March 2018 / Accepted: 31 July 2018

Abstract
Active and pH-sensitive nano-fillers were prepared from natural and modified montmorillonite (Mnt) and nanopackaged with anthocyanins extracted from the Jamaica (*Hibiscus sabdariffa*) flower. These were then used to reinforce corn (*Zea mays*) starch-based films plasticized with glycerol, and processed by extrusion and thermo-molding. Seven film systems were investigated for their potential as "active and intelligent" (A&I) bionanocomposite films with improved properties. The thermal and mechanical properties of the bionanocomposite films obtained were enhanced largely due to the added modified clay nano-fillers, and the nanopackaging of the anthocyanins between the nano-clay layers. Unfortunately, however, the bionanocomposite films failed as A&I materials, despite the supposed effect of the nano-clays as protective nano-encapsulating materials for the active and pH-sensitive compound (anthocyanins). The results obtained suggest that the exfoliation of the nano-fillers as a consequence of the shear forces inside the extruder led to the exposure of the anthocyanins during extrusion. Because of this, we consider the large-scale development of A&I biodegradable films incorporating natural pigments very unlikely being processed by extrusion/thermo-molding, since there are several significant processes involved in the techniques currently available in the food and polymer industries that leave the active and pH-sensitive compounds unprotected.

Keywords Food packaging · Mechanical properties · Nanopackaging · Thermoplastic starch

Introduction

The concept of food packaging has evolved over time as it has adapted to the changing needs of the world, and since the boom of the petrochemical industry in the early twentieth century has been manufactured mainly from synthetic polymers (Risch 2009). Food packaging made from synthetic polymers initially offered many advantages as it protects food from environmental conditions, while being inert to the food itself. However, since the 1980s, there has been a great deal of concern worldwide regarding the growth of the world population, and the effect of this on the use and disposal of a huge amount of food packaging materials made from synthetic polymers, which are unfriendly to the environment (Risch 2009). Because of this, during the last three decades, the use of starch as a biopolymeric matrix for the development of food packaging has been investigated, as it is readily available, economical, renewable, biodegradable, and can be processed by machinery currently available in both the polymer and food industries (Gutiérrez and Alvarez 2018). Corn starch (*Zea mays*) has attracted special attention due to its high levels of production worldwide (Gutiérrez et al. 2015). Nonetheless, in general, starch as a thermoplastic material has some drawbacks that must be solved, such as its tendency to adsorb moisture from the environment and its brittleness (Iman and Maji 2012).

✉ Tomy J. Gutiérrez
tomy.gutierrez@fi.mdp.edu.ar; tomy_gutierrez@yahoo.es

[1] Grupo de Polímeros, Departamento de Ciencia de los Materiales, Universidad Simón Bolívar (USB), Apartado 89000, Caracas 1080-A, Venezuela

[2] Grupo de Materiales Compuestos Termoplásticos (CoMP), Instituto de Investigaciones en Ciencia y Tecnología de Materiales (INTEMA), Facultad de Ingeniería, Universidad Nacional de Mar del Plata (UNMdP) y Consejo Nacional de Investigaciones Científicas y Técnicas (CONICET), Colón 10850, B7608FLC Mar del Plata, Argentina

Published online: 07 August 2018

In order to address these two problems, several alternatives have been put forward: (1) the use of different plasticizers, (2) the use of food additives, (3) modifying the starch itself, (4) mixing the starch with other natural or synthetic polymers, and (5) adding natural or modified nano-fillers obtained from cellulose, inorganic nanoparticles, and/or clays (Álvarez et al. 2017). Regarding this last item, although many authors have evaluated films derived from starch containing natural or modified nano-clays from montmorillonite (Mnt) that act as nano-fillers (Vazquez et al. 2012; Pérez et al. 2013), only one study conducted by our research group has been done with pH-sensitive nano-clays included in a thermoplastic starch (TPS) matrix (Gutiérrez and Alvarez 2018).

In the study mentioned, our research group aimed to develop "active and intelligent" (A&I) bionanocomposite films by incorporating active and pH-sensitive nano-fillers made from natural or modified Mnt into a TPS matrix, with and without added anthocyanins extracted from blueberries, using extrusion as the processing technique (Gutiérrez and Alvarez 2018). We hoped that this combination would result in pH-sensitive bionanocomposite films with improved properties, since as indicated above (1) the use of nano-clays as a reinforcement material has already been shown to reduce moisture absorption and brittleness, and (2) anthocyanins change color under different pHs due to a shift in their molecular structure from a quinoidal to a flavylium form (Gutiérrez et al. 2017). Unfortunately, we did not obtain the desired material due to two fundamental problems: (1) the pigment (anthocyanin, active and pH-sensitive compound) was degraded during the extrusion process, and (2) although the nano-clays used to nano-encapsulate the anthocyanins could theoretically protect them from the processing conditions, the exfoliation of these nano-fillers left the anthocyanins exposed. This lead us to believe that there must be a way to set the extrusion conditions that guarantees the complete exfoliation of the nano-clays and complete starch gelatinization, while maintaining the anthocyanins protected (Gutiérrez and Alvarez 2018).

With this in mind, in this study, we processed the films under smoother conditions compared to the previous study as follows: the screw torque speed of the extruder was reduced from 30 to 20 Hz; the extrusion temperature profile was slightly lowered from 90/100/105/110/120/120 °C to around 100 °C (90/100/105/110/110/110 °C), and the thermo-molding temperature of the material was reduced from 130 to 120 °C. In addition, new nano-clay systems were employed as nano-encapsulation materials to protect the anthocyanins extracted from Jamaica (*Hibiscus sabdariffa*) flowers before incorporating them into the TPS matrix (Gutiérrez et al. 2018). It is also worth mentioning that we did not find any record in the published literature of anthocyanins being obtained from Jamaica flowers.

Anthocyanins are susceptible to both oxidation and thermal degradation. However, this active and pH-sensitive compound (pigment) has been successfully used in the development of pH-sensitive (intelligent) films by the casting methodology, which reaches temperatures close to 100 °C in the film-forming solution (FFS) (Yoshida et al. 2014; Luchese et al. 2015; Pereira et al. 2015; Ma and Wang 2016; Choi et al. 2017; Liu et al. 2017; Gutiérrez 2018; Luchese et al. 2018). Nevertheless, directly incorporating anthocyanins into the TPS matrix does not produce pH-sensitive food packaging when an industrially scalable process such as extrusion is used (Gutiérrez and Alvarez 2018). This agrees with studies done by Altan et al. (2009) who demonstrated that food pigments are degraded under extrusion conditions. Because of this, we did not incorporate the anthocyanins directly into the TPS matrix.

As already mentioned above, other authors have obtained pH-sensitive materials through the casting methodology. This is unfeasible for the development of food packaging on a large scale, however, as it involves the use of large quantities of solvent (water) that must then be evaporated (Chevalier et al. 2018; Gutiérrez and Alvarez 2017a, 2018). This increases the energy consumption, and the large volumes of FFS required for production at an industrial level, thus goes against the need to develop green technologies and materials. For these reasons, food packaging manufacturers prefer the extrusion process (Xie et al. 2013). Nonetheless, the development of starch-based films by extrusion represents a challenge, as their production from native or modified starch is complex and involves several transitions such as granule expansion, gelatinization, melting, decomposition, and starch retrogradation (starch recrystallization) (Li et al. 2011; von Borries-Medrano et al. 2016; Xie et al. 2017).

The development of A&I food packaging materials is in line with the current concept of food packaging, i.e. that the packaging materials should extend food shelf-life while maintaining and monitoring safety and quality (Gutiérrez 2018). The old concept of food packaging where the material does not interact with the food and the packaging is merely an inert barrier that protects the food from external contaminants is already in disuse. According to Gutiérrez (2018), the use of A&I packaging also represents a promising alternative to help avoid the large amounts of post-harvest food losses. This food could then be used to feed the more than 842 million of people that still suffer from chronic hunger worldwide today (FAO 2012).

The aim of this study was to obtain A&I (pH-sensitive) bionanocomposite films with improved properties. To this end, we studied and analyzed the structural, barrier, mechanical, and antioxidant properties of bionanocomposite films prepared by extrusion from corn starch with incorporated A&I nano-fillers.

Experimental

Materials

Corn starch (*Zea mays*), glycerol, and several montmorillonites (Mnt) were used as the carbohydrate polymer, plasticizer, and nano-fillers, respectively, for the preparation of the bionanocomposite films. Corn starch was purchased from the Distribuidora Dos Hermanos, Mark Ying Yang (Mar del Plata, Argentina). Glycerol was obtained from Aurum (Mar del Plata, Argentina). The nano-clays used as nano-fillers in this study were natural Mnt (NMnt, or HPS according to the manufacturer), Mnt modified with dimethyl benzylhydrogenated tallow ammonium (MntMB, denominated 43B by the manufacturer), and Mnt modified with dimethyl dihydrogenated tallow ammonium (MntMD, or 72T according to the manufacturer). All the nano-clays were supplied by Laviosa Chimica Mineraria S.p.A. (Livorno, Italy) and were used as received. Following the manufacturer's descriptions, the modified Mnt are nano-clays prepared from a naturally occurring Mnt, purified and modified with quaternary ammonium salts (dimethyl benzylhydrogenated tallow ammonium and dimethyl dihydrogenated tallow ammonium). Jamaica (*Hibiscus sabdariffa*) flower extract (100% anthocyanin) was obtained according to the procedure described by Gutiérrez et al. (2018). Briefly, dehydrated flowers were purchased from a local market in the Ciudad Autónoma de Buenos Aires, Provincia de Buenos Aires, Argentina. The flowers are marketed by an Argentine company and labeled as harvested in the Jardín America (Street Amado Nervo 478, Provincial de Misiones, Argentina; geographical coordinates—latitude S 27° 2′ 25.597″ and longitude W 55° 14′ 22.906″). The Jamaica flowers were weighed (30 g) and then immersed in 200 mL of ethanol (Aldrich—product code: 34923), applying a slight pressure on the immersed flowers in order to extract the pigment (anthocyanin). The extract was then decanted to remove the solid fragments of the flower petals. The Jamaica flower extract (JFE) was prepared the same day the nano-clays were developed, and maintained under refrigeration at 5 °C in a dark container until further processing in order to avoid oxidative damages.

Formation of the Nano-Fillers

The nano-fillers with added JFE were prepared by mixing 20 g of each nano-clay used with 50 mL of JFE. The mixture was then frozen at − 20 °C for 48 h after which it was lyophilized at 13.33 Pa (100 mTorr) and then frozen again at − 50 °C for 72 h using a Gland type Vacuum Freeze Dryer, Columbia International, Model FD-1B-50 (Shaan Xi, China) in order to obtain a solvent-free product. Lyophilization also preserves the active compound (anthocyanin) in the JFE and ensures a size of clay particle in the nanometer range. The resultant nano-clays were conditioned in containers with a saturated solution of NaBr (a_w ~0.575 at 25 °C) for 7 days before preparing the bionanocomposite films in order to maintain controlled and known conditions. During this period, the containers were protected from light in a dark room to avoid the photodegradation of the pigment. Six types of nano-fillers were prepared as follows: natural Mnt (NMnt), natural Mnt containing JFE (NMnt + JFE), Mnt modified with dimethyl benzylhydrogenated tallow ammonium (MntMB), Mnt modified with dimethyl benzylhydrogenated tallow ammonium containing JFE (MntMB + JFE), Mnt modified with dimethyl dihydrogenated tallow ammonium (MntMD), and Mnt modified with dimethyl dihydrogenated tallow ammonium containing JFE (MntMD + JFE). These nano-fillers have already been exhaustively characterized by our research group in Gutiérrez et al. (2018).

Film Formation and Extrusion Conditions

Bionanocomposite films were made from native corn starch using a 120:280 (g/g) ratio (glycerol:starch). To evaluate the effects of each filler (NMnt, NMnt + JFE, MntMB, MntMB + JFE, MntMD, and MntMD + JFE) on the properties of the resulting films, 16 g (4% *w*/*w*) of each was added to the starch content of each film system, maintaining the same glycerol:starch ratio. This percentage was employed based on previous studies carried out by our research group (Vazquez et al. 2012; Ludueña et al. 2015): percentages greater than 4% *w*/*w* can deteriorate the mechanical properties of the developed materials. Each system was pre-blended manually until homogeneous mixtures were obtained. The mixtures were then processed by extrusion in a twin-screw extruder (doble A Argentina) with six heating zones. The temperature profile used was 90/100/105/110/110/110 °C with a screw rotation speed of 20 Hz and a feed rate of 15 g/min. All the mixtures were processed under constant conditions. After processing, the materials obtained from the extruder were allowed to cool to room temperature (25 °C) before being pelletized using an automatic pelletizer (Weinuo Technology Co., Ltd., Jiangsu, China). The pellets (90 g per film system) were then hot-pressed using a hydraulic press (Proflow, Mar del Plata, Argentina) at 120 °C and 1×10^7 Pa (100 bar) for 20 min, after which a cooling cycle was applied until they reached a temperature of 30 °C. The seven resulting materials were thermoplastic starch (TPS), TPS + NMnt, TPS + NMnt + JFE, TPS + MntMB, TPS + MntMB + JFE, TPS + MntMD, and TPS + MntMD + JFE. Finally, the prepared films were conditioned at a controlled relative humidity (~57%) for a week at 25 °C before characterization.

Film Characterization

Thermogravimetric Analysis (TGA)

The thermogravimetric tests were carried out using a thermal analyzer (Model TGA Q500, Hüllhorst, Germany). Samples were heated at a constant rate of 10 °C/min from room temperature up to 600 °C under a nitrogen flow of 30 mL/min. Film weights were in the range of 17–29 mg. Three replicates per sample were analyzed to ensure repeatability. Standard deviations (SD) were lower than 1% for all the systems tested, and the representative curves of each one were reported.

X-Ray Diffraction (XRD)

A PAN analytical X'Pert PRO diffractometer (Netherlands) equipped with a monochromatic Cu K_α radiation source ($\lambda = 1.5406$ Å) operating at a voltage of 40 kV, current 40 mA, and scanning rate 1°/min was used to obtain the X-ray diffractograms of the films studied. The scanning region of the samples was in a 2θ range between 3° and 33°. The distances between the planes of the crystals d (Å) were calculated from the diffraction angles (°) measured from the X-ray diffractograms according to Bragg's law:

$$n\lambda = 2d\sin(\theta) \tag{1}$$

where λ is the Cu K_α radiation wavelength and n is the order of reflection. For the calculations, n was taken as 1. The thicknesses of the samples on the slides were ~0.95 mm.

Determination of Film Thickness (*e*)

The thickness (e) of each bionanocomposite film system was determined by measuring samples at 18 different locations per sample using a micrometer (Liuling, Shanghai, China) with an accuracy of ± 0.001 mm. Results were reported as average values ± SD.

Water Vapor Permeability (WVP)

Water vapor permeability was measured following the desiccant method proposed in ASTM E96-00e1 (2000). Briefly, 4.9 cm diameter discs of each film system were used to seal the open mouths of test capsules (exposed area ~18.86 cm^2) containing anhydrous calcium chloride ($CaCl_2$, 0% relative humidity). The test capsules were then introduced into a controlled relative humidity chamber (65 ± 1%) at 25 °C, and weighed daily with an analytical balance (± 0.0001 g) over a period of 5 days. Weight gain (g) was plotted against time (h) to measure the water vapor transmission rate (WVTR). The WVTR (g/h m^2) was then determined by dividing the weight gain vs time slope by the exposed film area (m^2), and the WVP of each film system was calculated as follows:

$$\mathrm{WVP} = {}^{G\ x\ e}/_{S\ x\ \mathrm{RH}\ x\ t\ x\ A} \tag{2}$$

where G is the mass gained, e the thickness of the film, S the saturated vapor pressure at 25 °C, RH the relative humidity, t time, and A the exposed area of each sample. Measurements were made after an initial equilibration period to ensure steady-state diffusion, and at least five were taken for each sample. All assays were performed in triplicate, reporting the average and SD in each case.

Opacity

The opacity of the films was determined following the methodology described by Gutiérrez (2017). The ultraviolet (UV) and visible light barrier properties of the films were measured using a UV-Vis spectrophotometer (u-2001, Japan) at selected wavelengths between 400 and 800 nm. Film opacity was then calculated at 600 nm using the equation given by Han and Floros (1997):

$$\mathrm{Opacity} = {}^{A_{600}}/_{e} \tag{3}$$

where A_{600} is the absorbance at 600 nm and e is the film thickness (mm).

Water Solubility (WS)

Three replicates of each film system were cut into 12 mm-diameter discs. The initial dry matter content (W_i) of each film type was then determined by drying the discs to a constant weight in an oven (Memmert, Germany) at 105 °C for 24 h. Each sample was then immersed in 50 mL of distilled water and kept at 25 °C for 24 h. The insoluble portions of the film samples were separated from the soluble matter in the water and dried in an oven at 105 °C for 24 h. The oven-dried samples were then reweighed to measure the weight of the unsolubilized dry matter (W_f). The data obtained was used to calculate the WS for each film system using Eq. 4:

$$\mathrm{WS}\ (\%) = \frac{(W_i - W_f)}{W_i}\ \mathrm{x}\ 100 \tag{4}$$

Scanning Electron Microscopy (SEM)

The morphological analysis of the cryo-fractured surfaces of the bionanocomposite films was done using a JEOL JSM-6460 LV scanning electron microscope. Film samples were cryo-fractured by freezing them in liquid nitrogen and their morphologies were then observed in the

fracture cross-section of the films. For the analyses, films were mounted on bronze stubs and sputter-coated (Sputter coater SPI Module, Santa Clara, CA, USA) with a thin layer of gold for 35 s and observed with an accelerating voltage of 15 kV.

Uniaxial Tensile Tests

At least 20 specimens of each film system were cut in a bone-shape with an effective area of ~28.6 mm long × ~5.5 mm width and cross-sectional area ~6.5 mm^2 (the exact values differed slightly between samples). They were then divided into two groups of 10 samples each per film system in order to determine the mechanical properties of the films at two constant speeds: 1 and 5 mm/s, selected following ISO 527-2 (2012). Specimens were mounted and clamped with tensile grips (A/TG model), and then tested at 25 °C until they broke. An INSTRON 4467 machine was used to obtain the force-distance curves following the ISO 527-2 (2012) norm. The mechanical properties at break: maximum stress (σ_m) and strain at break (ε_b) were obtained from the stress-strain curves. The stress-strain curves were obtained from the stress-distance curves as outlined in ISO 527-2 (2012). Young's modulus (E) was then determined from the linear regression slope of the stress-strain curves, and toughness (T) was calculated from the area underneath them.

Antioxidant Activity

The antioxidant capacity was determined by the 2,2-diphenyl-1-picrylhydrazyl radical (DPPH•) method (Rincón et al. 2003), which is based on the reduction of the DPPH• radical by the antioxidants contained in a sample. The DPPH• radical is stable in a 0.025 g/L ethanol solution and has a purple color, which is progressively lost as the sample containing antioxidants is added. Radical bleaching was determined at 515 nm and antioxidant activity was quantified using a Trolox calibration curve (water-soluble analogue of vitamin E). This method reflects the activity of antioxidant compounds, which are capable of donating protons for scavenging DPPH• radicals (Miller and Rice-Evans 1997). Analyses were done using ~0.25 g of each sample mixed with 975 μL of a DPPH• solution (60 μmol in methanol). Absorbance was measured immediately (time 0) and again after 30 min. The results were expressed as percentages of inhibition.

$$\text{Inhibition } (\%) = {}^{A_0 - A_{30}}/_{A_0} \text{ x } 100 \quad (5)$$

where A_o is the absorbance at time 0 and A_{30} is the absorbance after 30 min.

Response to pH Changes

Three samples of each film system were cut into 12 mm-diameter discs, and then submerged separately in Petri dishes containing 20 mL of a solution at a pH equal to either 1 (0.1 M HCl solution), 7 (distilled water), or 13 (0.1 M NaOH solution). Film response was then evaluated from images taken with an 8.1 M pixel Cyber-shot Sony camera; model DSC-H3 (Tokyo, Japan). This was done in order to evaluate the potential pH-sensitive effect of the bionanocomposite films containing the JFE.

Statistical Analyses

The OriginPro 8 (Version 8.5, Northampton, USA) software was used to perform an analysis of variance (ANOVA) for the data obtained from each test conducted. Results were shown as average values ± SD. Differences between the mean values of the measured properties were compared using a multiple-range Tukey's test. A significance level of 0.05 was used.

Results and Discussion

Thermogravimetric Analysis (TGA)

A thermogravimetric analysis of the films developed (see TGA curves, Fig. 1) was carried out in order to analyze the thermal stability of these materials, as well as to test for possible phase separation due to incompatibility between the thermoplastic starch (TPS) and the clay nano-fillers. According to the published literature (Moreno et al. 2017), TPS-based films containing glycerol as a plasticizer thermally degrade in three stages. Stage one occurs between 50 and 100 °C, and is related to the evaporation of water absorbed from the environment and free water contained within the material. Stage two is associated with the evaporation of the glycerol-rich phase which occurs from 160 °C with a maximum evaporation temperature at 290 °C. It should be noted that during this stage, part of the starch contained in the glycerol-rich phase also decomposes. The third and last stage of thermal degradation takes place from 300 to 320 °C when the starch-rich phase is decomposed. According to Zeppa et al. (2009), the mechanism of degradation in this phase is the elimination of the starch polyhydroxyl groups, as well as the depolymerization and decomposition of the TPS matrix, followed by the production of carbon.

As expected, all the bionanocomposite films had a higher residual mass content (between 10.96 and 15.11%) than the TPS film (7.54%) after the last stage of thermal degradation. This is logical since the clay nano-fillers within the TPS matrix contribute to an increase in the residual mass as the montmorillonite (Mnt) itself does not decompose during this stage.

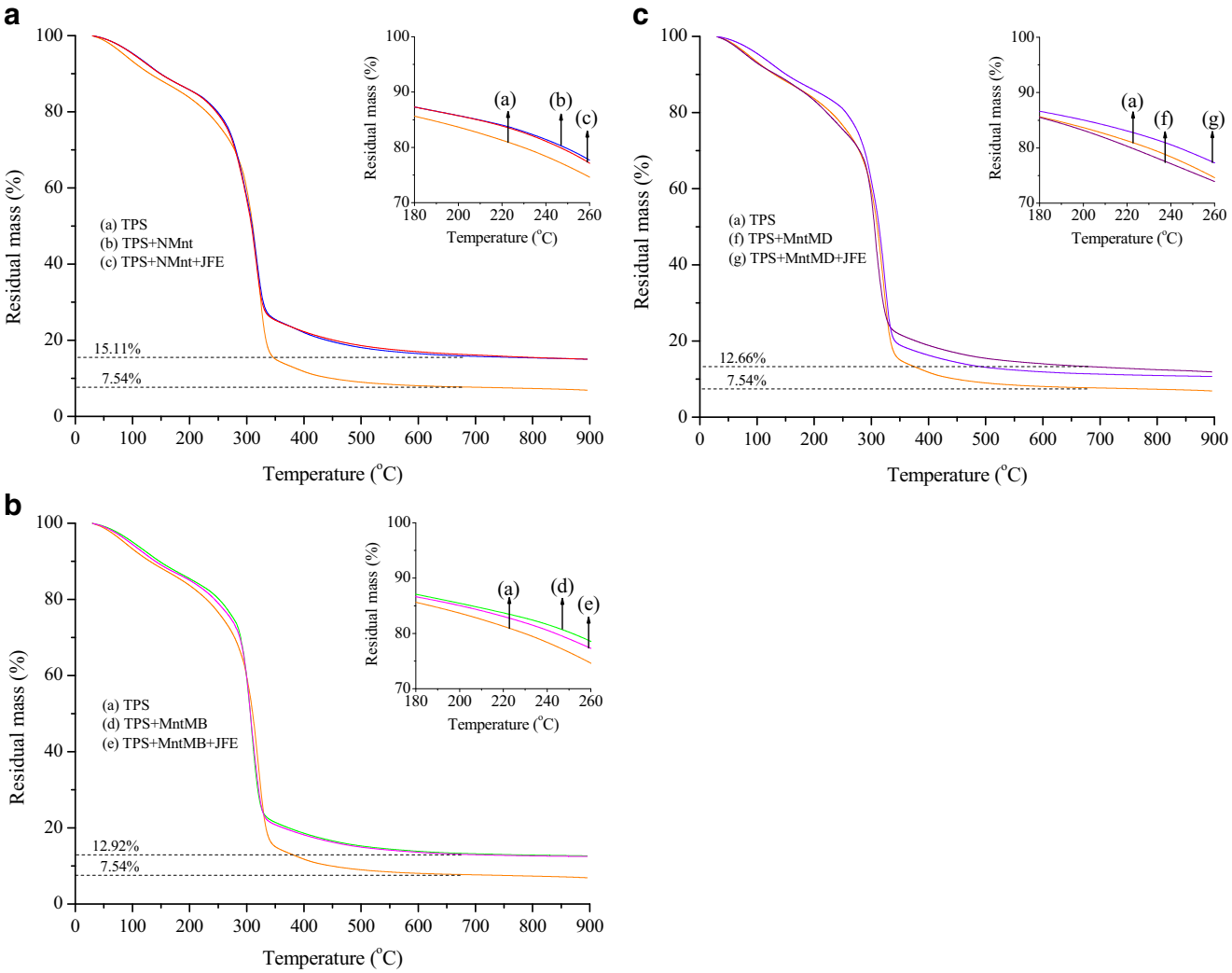

Fig. 1 TGA curves of the different films studied: **a** thermoplastic starch (TPS), **b** TPS + natural montmorillonite (TPS + NMnt), **c** TPS + natural montmorillonite containing Jamaica flower extract (TPS + NMnt + JFE), **d** TPS + montmorillonite modified with dimethyl benzylhydrogenated tallow ammonium (TPS + MntMB), **e** TPS + montmorillonite modified with dimethyl benzylhydrogenated tallow ammonium containing Jamaica flower extract (TPS + MntMB + JFE), **f** TPS + montmorillonite modified with dimethyl dihydrogenated tallow ammonium (TPS + MntMD), and **g** TPS + montmorillonite modified with dimethyl dihydrogenated tallow ammonium containing Jamaica flower extract (TPS + MntMD + JFE)

Specifically, the order of residual mass content (from high to low) for the bionanocomposite films studied after the last thermal degradation stage was as follows: TPS + NMnt (15.11%) = TPS + NMnt + JFE (15.11%) > TPS + MntMB (12.92%) = TPS + MntMB + JFE (12.92%) > TPS + MntMD (12.66%) > TPS + MntMD + JFE (10.96%). This order is possibly closely related to the organic mass content decomposed from the chemically organo-modified clays (organo-clays) within the TPS matrix. It is worth remembering that the organo-clays (MntMB, MntMB + JFE, MntMD, and MntMD + JFE) did contain organic matter from the organo-modifying agents of the clays, whereas the natural (unmodified) nano-fillers (NMnt and NMnt + JFE) did not. Thus, the lower residual mass content in the bionanocomposite films containing the organo-clays (TPS + MntMB, TPS + MntMB + JFE, TPS + MntMD, and TPS + MntMD + JFE) compared to the natural clays (TPS + NMnt and TPS + NMnt + JFE) can be presumed to be the product of a mass loss, which could be a consequence of the decomposition of the organic matter in these clays. From this, it can be further inferred that the MntMD and MntMD + JFE clays had a higher organic material content than the MntMB and MntMB + JFE clays. The modifying agents for the MntMB and MntMD organo-clays were dimethyl benzylhydrogenated tallow ammonium and dimethyl dihydrogenated tallow ammonium, respectively. Thus our first conclusion is that the organo-modifying agent with the lower volume and molecular weight (dimethyl dihydrogenated tallow ammonium) can enter between the layers of the nano-clays more easily, thus contributing more organic matter content than the organo-modifying agent with the higher volume

and molecular weight (dimethyl benzylhydrogenated tallow ammonium). In summary, the bionanocomposite films containing the nano-clays with a greater organic content within their layers showed a lower residual mass after the last stage of thermal degradation. This analysis is in line with the exhaustive characterization of these nano-clays recently reported by Gutiérrez et al. (2018).

From Fig. 1 (see box at the top right of each panel), it can also be observed that all the nano-fillers tested increased the thermal resistance of the bionanocomposite films in the glycerol rich phase, with the exception of the TPS + MntMD + JFE film. These results suggest that the nano-fillers and TPS matrix interacted positively with glycerol, thus retarding its evaporation. This effect was more significant in the bionanocomposite films containing the Jamaica flower extract (JFE) compared those that did not. This can be explained by the hydrogen bond interactions between the JFE nanopackaged within the nano-clays and the glycerol. In addition, the nano-fillers with added JFE showed a greater interlayer spacing compared to their analogues without JFE (Gutiérrez et al. 2018). Thus, wider interlayer spacing between the nano-clays leads to stronger nano-filler/glycerol interactions.

To conduct a more in-depth analysis of the data, derivative TGA (DTGA) curves were plotted for each film system (Fig. 2). The first notable result was that the decomposition temperatures of the starch-rich phase were found to be around 321 °C for all the films tested (see Fig. 2a). Similar results were obtained by Romero-Bastida et al. (2016) for native and high amylose starch films containing natural Mnt. In particular, the thermal degradation temperature of the starch-rich phase of the bionanocomposite films containing the natural nano-fillers (TPS + NMnt and TPS + NMnt + JFE) was equal to that of the TPS matrix (see Fig. 2b) demonstrating that these nano-fillers did not have a significant effect on the starch-rich phase. However, the thermal degradation temperatures of the starch-rich phase were lower in the TPS + MntMB, TPS + MntMB + JFE, and TPS + MntMD bionanocomposite films than the TPS, TPS + NMnt, and TPS + NMnt + JFE films. This suggests that the MntMB, MntMB + JFE, and MntMD nano-fillers impede starch-starch interactions to a greater degree than the natural nano-fillers (NMnt and NMnt + JFE) and the TPS matrix by interacting with the starch chains themselves. This is possibly a consequence of the wider interlayer spacing between the organo-clay nano-fillers (MntMB—18.5 Å, MntMB + JFE—20.8 Å, and MntMD—26.5 Å) compared to the natural nano-fillers (NMnt—12.5 Å and NMnt + JFE—12.5 Å) (Gutiérrez et al. 2018). Our second conclusion is thus that clay nano-fillers with wider interlayer spacing prevent starch-starch interactions, while improving starch/nano-filler and glycerol/nano-filler interactions. This is in line with other similar studies carried out by our research group (Gutiérrez and Alvarez 2018).

The TPS + MntMD + JFE film proved to be an exception to the above argument, as the degradation temperature of the starch-rich phase showed an increase compared to the TPS film. The use of the MntMD + JFE nano-filler thus led to undesirable results, i.e. there are more and stronger hydrogen bond interactions between the starch-starch chains than those between the starch/nano-filler and glycerol/nano-filler. This means that the starch within the TPS matrix may have undergone recrystallization (starch retrogradation). We could thus speculate that the MntMD + JFE nano-filler may serve as a core for starch recrystallization. More information about the crystallinity of the developed films will be analyzed in the following section ("X-ray diffraction" section).

The DTGA curves (see Fig. 2b) also show that the starch and the nano-fillers are slightly incompatible in the TPS + NMnt, TPS + NMnt + JFE, and TPS + MntMD + JFE bionanocomposite films. This is demonstrated by the slight phase separation that can be observed for the peak around 290 °C, and may be attributed to the evaporation temperature of the glycerol. A homogeneous material should degrade in a single step, i.e. the DTGA curves should show a single thermal degradation peak. This did not occur in the TPS + NMnt, TPS + NMnt + JFE, and TPS + MntMD + JFE films, thus suggesting that these materials are far more anisotropic than the TPS + MntMB, TPS + MntMB + JFE, and TPS + MntMD films. Phase separation in the TPS + NMnt, TPS + NMnt + JFE, and TPS + MntMD + JFE films also means that the glycerol is free or available. Our third conclusion is thus that clay nano-fillers with greater interlayer spacing prevent phase separation, resulting in homogeneous bionanocomposite carbohydrate polymers, i.e., polymers with well dispersed nano-fillers within the TPS matrix.

During the thermal degradation stage associated with the evaporation of water adsorbed from the environment (stage 1), the following increasing order of maximum temperature for water evaporation to occur was observed: TPS + MntMD (77.50 °C) < TPS (88.89 °C) < TPS + MntMB + JFE (112.99 °C) < TPS + MntMB (122.46 °C) < TPS + NMnt + JFE (128.24 °C) < TPS + NMnt (131.57 °C) = TPS + MntMD + JFE (131.57 °C). Interestingly, the three film systems with higher water evaporation temperatures (TPS + NMnt, TPS + NMnt + JFE, and TPS + MntMD + JFE) were the same ones that showed a slight phase separation. This suggests that phase separation gives materials that are more susceptible to water, since free glycerol can be a water receiver.

X-Ray Diffraction (XRD)

The X-ray diffractograms (Fig. 3) of the developed films were taken mainly to investigate the structures adopted by the clay nano-fillers within the TPS matrix, i.e. exfoliation, intercalation, and/or agglomeration (Rhim and Kim 2014). The X-ray diffractograms of all the films studied showed that they

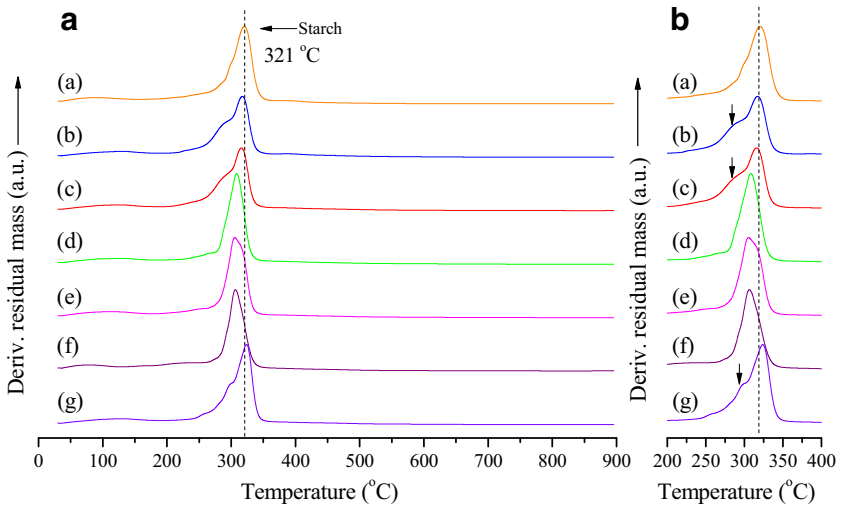

Fig. 2 **a** DTGA curves of the different films studied in all the temperature range evaluated. **b** DTGA curves of the different films studied in the temperature range of 200 to 400 °C. Film systems: (a) thermoplastic starch (TPS), (b) TPS + natural montmorillonite (TPS + NMnt), (c) TPS + natural montmorillonite containing Jamaica flower extract (TPS + NMnt + JFE), (d) TPS + montmorillonite modified with dimethyl benzylhydrogenated tallow ammonium (TPS + MntMB), (e) TPS + montmorillonite modified with dimethyl benzylhydrogenated tallow ammonium containing Jamaica flower extract (TPS + MntMB + JFE), (f) TPS + montmorillonite modified with dimethyl dihydrogenated tallow ammonium (TPS + MntMD), and (g) TPS + montmorillonite modified with dimethyl dihydrogenated tallow ammonium containing Jamaica flower extract (TPS + MntMD + JFE)

exhibited behavior typical of semicrystalline materials, i.e. they were mainly amorphous with a weak crystalline phase. Similar results have been reported elsewhere for other starch-based films (Slavutsky et al. 2012; Abreu et al. 2015; Wilpiszewska et al. 2015).

The characteristic peaks of the crystalline phase of the starch at $2\theta = 12.9°$, 16.9°, 19.6°, and 22.4°, corresponding to the *d*-spacings ≅ 6.9, 5.2, 4.5, and 4.0 Å, respectively, were observed (see Fig. 3a). The peaks at $2\theta = 16.9°$ and 22.4° are typical of the A-type structure frequently observed in cereal-based materials such as corn starch (Vasanthan and Hoover 1992), used in this study as the carbohydrate polymer matrix. According to García-Tejeda et al. (2013) $2\theta = 16.9°$, corresponding to *d*-spacing ≅ 5.2 Å, is associated with interactions

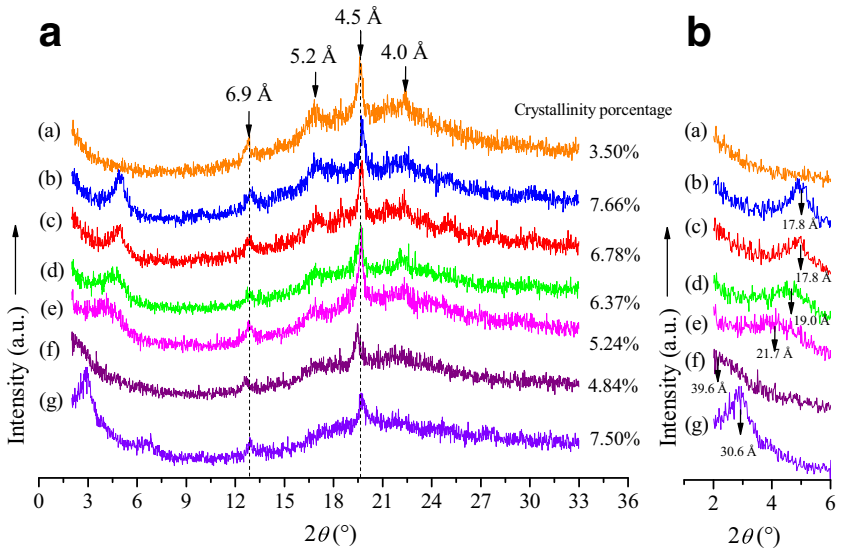

Fig. 3 **a** X-ray diffraction diffractograms in the range of 2–33° (2θ) and crystallinity percentages of the different films studied. **b** X-ray diffraction diffractograms in the range of 2–6° (2θ) of different films. Film systems: (a) thermoplastic starch (TPS), (b) TPS + natural montmorillonite (TPS + NMnt), (c) TPS + natural montmorillonite containing Jamaica flower extract (TPS + NMnt + JFE), (d) TPS + montmorillonite modified with dimethyl benzylhydrogenated tallow ammonium (TPS + MntMB), (e) TPS + montmorillonite modified with dimethyl benzylhydrogenated tallow ammonium containing Jamaica flower extract (TPS + MntMB + JFE), (f) TPS + montmorillonite modified with dimethyl dihydrogenated tallow ammonium (TPS + MntMD), and (g) TPS + montmorillonite modified with dimethyl dihydrogenated tallow ammonium containing Jamaica flower extract (TPS + MntMD + JFE)

between the short external amylopectin chains and the glycerol. The peaks with *d*-spacing ≅ 4.5 and 6.9 Å observed in the films are indicative of a V-type structure, and are associated with glycerol-starch hydrogen bonding interactions (Gutiérrez and Alvarez 2018).

The interlayer spacing (d_{001}) of the nano-clays within the TPS matrix can be observed from the X-ray diffractograms in the region between 2° and 6° (Fig. 3b) (Gutiérrez et al. 2018). The diffraction peaks at 5.0° (17.8 Å) observed for the TPS + NMnt and TPS + NMnt + JFE films reveals that the NMnt and NMnt + JFE nano-fillers underwent exfoliation (expansion of their layers) during extrusion, since both nano-fillers showed diffraction peaks at 7.1° (12.5 Å) before this process was carried out (Gutiérrez et al. 2018). However, the diffraction peaks also suggest that the NMnt and NMnt + JFE nano-fillers are intercalated within the TPS matrix, and thus must be partially exfoliated and partially interleaved within it. The partially exfoliated structure demonstrates that there were only a few starch chains between the interlayer spacing of the nano-fillers, and thus that the interactions between them and the starch were limited.

On the other hand, the MntMB and MntMB + JFE organo-clays (both with and without JFE) showed a greater degree of exfoliation within the TPS matrix than the natural nano-fillers (NMnt and NMnt + JFE). Thus, the modification of nano-clays with dimethyl benzylhydrogenated tallow ammonium favors their exfoliation. The results suggest that the greater exfoliation of the nano-fillers organo-modified with dimethyl benzylhydrogenated tallow ammonium (MntMB and MntMB + JFE) enables them to interact more with the TPS matrix than the natural nano-fillers used (NMnt and NMnt + JFE). In addition, the MntMB + JFE nano-filler was also more exfoliated within the TPS matrix than the MntMB nano-filler (without JFE). These results are in line with the analysis of the DTGA curves.

It was also observed that the MntMD nano-filler was almost totally exfoliated within the TPS matrix. This means that it interacts the most strongly with the TPS matrix of all the nano-fillers used. This was demonstrated by the X-ray diffractograms which showed that the diffraction peak corresponding to this nano-filler in the region between 2° and 6° was almost nonexistent. Thus, the organo-modification with dimethyl dihydrogenated tallow ammonium resulted in a greater degree of exfoliation of the nano-clay during the extrusion process than the organo-modification with dimethyl benzylhydrogenated tallow ammonium. This may be due to the molecular weight and volume of the organo-modifying agent. Dimethyl dihydrogenated tallow ammonium has a lower weight and molecular volume than dimethyl benzylhydrogenated tallow ammonium, and can thus enter more easily into the interlayer spacing (galleries) of the nano-clays. This results in a greater number of molecules of the modifying agent in the nano-clay galleries. The more molecules of the organo-modified agent there are in the galleries, the greater the expansive effect of the nano-clays (exfoliation), which is favored by the extrusion process. This fits well with the analysis of the TGA curves in the final stage of thermal degradation (see "Thermogravimetric analysis" section).

As regards the TPS + MntMD + JFE film, the incorporation of JFE into the MntMD nano-filler apparently does not increase the exfoliation process in the same way as it does when incorporated into the MntMB nano-filler. Nonetheless, we can speculate that JFE actually does favor the exfoliation process of both nano-fillers. However, this process is only beneficial up to the point where the exfoliated material does not reduce in particle size so much that the area/volume ratio increases to the extent that agglomeration of the nano-clays occurs. This could explain the phase separation observed from the DTGA curves for this film system (TPS + MntMD + JFE), where it was established that starch-starch interactions were more favored than starch/nano-filler interactions.

Table 1 shows the interlayer spacing (d_{001}) of the clay nano-fillers before and after the extrusion process. It can be seen that in all cases, the interlayer spacing (d_{001}) of the nano-fillers increased after extrusion, i.e. extrusion is an effective mechanical method that guarantees the exfoliation of the clay nano-fillers. It should be noted that this increase was most significant for the TPS + MntMD film, i.e. the TPS matrix containing the MntMD nano-filler.

From Fig. 3a, a slight shift from $2\theta \approx 12.9°$ to $2\theta \approx 19.6°$ was observed for the TPS + MntMD film. This demonstrates a slight increase in the molar volume that directly affects the V-type structure, i.e. the hydrogen bond interactions between the starch and glycerol. Similar results were reported by Gutiérrez and Alvarez (2017b) for eco-friendly films prepared from plantain flour/poly(ε-caprolactone) (PCL) blends under reactive extrusion conditions. According to Gutiérrez and Alvarez (2017b), this behavior is beneficial for obtaining starch-based thermoplastic materials with improved properties. This agrees with the results shown so far for the TPS + MntMD film.

In order to evaluate the orientation of the nano-fillers within the TPS matrix, the crystallinity percentages of the bionanocomposite films were calculated. It is worth noting that the crystallinity percentage obtained for the TPS film (3.5%) could be related to the residual crystallinity, which results from a very small fraction of starch granules that do not undergo complete granular disruption (i.e. do not become gelatinized or plasticized), as well as being a consequence of the parallel orientation of the starch chains, which leads to retrogradation (starch recrystallization) (Müller et al. 2011). As expected, all the bionanocomposite films had higher crystallinity values (> 4.78%) than the TPS film (3.5%). This is due to the intrinsic crystallinity of the clays used as nano-fillers within the TPS matrix.

Table 1 Interlayer spacing (d_{001}) of the clays used as nano-fillers of the thermoplastic starch (TPS) matrix before (d_i) and after (d_f) the extrusion process

Nano-filler systems	d_i (Å)[a]	d_f (Å)	Δd (Å)[b]
NMnt	12.5	17.8	5.3
NMnt + JFE	12.5	17.8	5.3
MntMB	18.5	19.0	0.5
MntMB + JFE	20.8	21.7	0.9
MntMD	26.5	39.6	13.1
MntMD + JFE	27.3	30.6	3.3

Nano-filler systems: natural montmorillonite (NMnt), natural montmorillonite containing Jamaica flower extract (NMnt + JFE), montmorillonite modified with dimethyl benzylhydrogenated tallow ammonium (MntMB), montmorillonite modified with dimethyl benzylhydrogenated tallow ammonium containing Jamaica flower extract (MntMB + JFE), montmorillonite modified with dimethyl dihydrogenated tallow ammonium (MntMD), and montmorillonite modified with dimethyl dihydrogenated tallow ammonium containing Jamaica flower extract (MntMD + JFE)

[a] The values of interlayer spacing (d_{001}) of the nano-clays used are found in Gutiérrez et al. (2018)

[b] Δd (Å) = d_f (Å) - d_i (Å)

An inverse relationship between the interlayer spacing of the nano-fillers and the crystallinity percentage values of the bionanocomposite films developed was found, i.e. the more exfoliated materials were less crystalline (more amorphous/more dispersed). This may be because the layers of nano-clays, once exfoliated, orientate randomly within the TPS matrix. In contrast, little exfoliated nano-clays maintain a parallel orientation within the TPS matrix, resulting in more crystalline bionanocomposite films. The TPS + MntMD + JFE film was more crystalline and with a lower interlayer spacing compared to their analogous film (TPS + MntMD). This provides further evidence to suggest that this nano-filler (MntMD + JFE) is partially agglomerated within the TPS matrix. The results discussed so far thus indicate that a more exfoliated nano-filler with a greater interlayer spacing within the TPS matrix improves nano-filler/starch interactions (thus avoiding phase separation and starch-starch interactions). This results in less crystalline and anisotropic materials, i.e. materials that are more amorphous/more dispersed/more homogeneous.

Thickness (e)

Thickness is an important variable that affects the following properties: water vapor permeability (WVP), opacity, density (ρ), and maximum stress (σ_m). The thickness values of the films developed in this study were not significantly different ($p \geq 0.05$, approx. 1.0 mm) (Table 2). This means that the properties indicated above (WVP, opacity, and σ_m) are not altered by the thickness in the film systems, and instead could be directly related to the chemical interactions occurring within the materials, as well as with the arrangement (orientation) of the nano-fillers within the TPS matrix.

Water Vapor Permeability (WVP)

One of the main advantages of bionanocomposite films compared to their analogous non-bionanocomposites is that the former give food packaging materials that are less permeable to water vapor, O_2, and CO_2 (Álvarez et al. 2017). This is a consequence of the modification of the transport properties of the thermoplastic materials obtained (Gutiérrez and Álvarez 2017). A reduction in WVP is positively related to an increase in the useful life of the foods packaged using these materials (Cazón et al. 2017). In this study, however, no statistically significant differences ($p \geq 0.05$) in WVP were observed between the TPS film and the bionanocomposite films developed.

Nevertheless, a statistically significant increase ($p \leq 0.05$) in the WVP value was observed for the TPS + MntMD film compared to the other bionanocomposite films containing the different nano-fillers without added JFE (TPS + NMnt and TPS + MntMB). It is worth remembering that the TPS + MntMD film was the material with the most exfoliated nano-filler. Previously in the literature, it has been suggested that bionanocomposite films with a greater degree of exfoliation and random dispersion make the path for the passage of gases more tortuous, thus reducing gas permeability values (Choudalakis and Gotsis 2009). Our results initially seem to conflict with this. Nonetheless, there are three main factors that affect the permeability of bionanocomposite films: the volume fraction of the nano-layers, their orientation relative to the diffusion direction, and their aspect ratio (Choudalakis and Gotsis 2009). In addition, it is generally accepted that the transport mechanism within starch-based films is governed by Fick's law (Choudalakis and Gotsis 2009). Thus, an increase in the WVP of the TPS + MntMD compared to the TPS + NMnt and TPS + MntMB films could be related to the parallel orientation of the MntMD nano-filler with respect to the passage of water vapor within the matrix, which would facilitate its WVP. Furthermore, the higher WVP value recorded for the TPS + MntMD film (compared to the TPS + NMnt and TPS + MntMB films) may be associated with the increase in the molar volume, observed from the XRD diffractograms for the same film system (TPS + MntMD, see "X-ray diffraction" section—Fig. 3a). This increase in molar volume would enable water vapor molecules to pass through the material more easily, thus increasing WVP.

The addition of JFE within the layers of the nano-fillers, compared to their analogues without JFE, did not produce, in general, statistically significant differences ($p \geq 0.05$) in WVP. An exception to this was the TPS + MntMB + JFE film which had a higher WVP value than the TPS + MntMB film. Apparently, the MntMB + JFE nano-filler has a more parallel

Table 2 Thickness (e), opacity, water vapor permeability (WVP), and water solubility (WS) of the different films

Parameter	TPS	TPS + NMnt	TPS + NMnt + JFE	TPS + MntMB	TPS + MntMB + JFE	TPS + MntMD	TPS + MntMD + JFE
e (mm)	0.9 ± 0.2a	0.9 ± 0.2a	0.9 ± 0.2a	1.0 ± 0.2a	1.0 ± 0.2a	1.0 ± 0.2a	1.0 ± 0.2a
WVP ($\times 10^{-5}$ g/m h Pa)	2.4 ± 0.5a	2.1 ± 0.2a	2.5 ± 0.3a,b	2.14 ± 0.08a	2.6 ± 0.1a,b,c	2.5 ± 0.1a,b,c	2.2 ± 0.9a
Opacity	1.556 ± 0.001a	2.983 ± 0.001f	2.563 ± 0.001e	1.757 ± 0.001b	1.970 ± 0.001c	1.757 ± 0.001b	2.273 ± 0.001d
WS (%)	25.5 ± 0.8b	24.3 ± 0.7b	29.4 ± 1.0e	26.1 ± 0.3b,c	30.6 ± 0.8e	22.9 ± 0.3a	27.6 ± 0.4d

Equal letters in the same row indicate no statistically significant differences ($p \leq 0.05$)

Film systems: thermoplastic starch (TPS), TPS + natural montmorillonite (TPS + NMnt), TPS + natural montmorillonite containing Jamaica flower extract (TPS + NMnt + JFE), TPS + montmorillonite modified with dimethyl benzylhydrogenated tallow ammonium (TPS + MntMB), TPS + montmorillonite modified with dimethyl benzylhydrogenated tallow ammonium containing Jamaica flower extract (TPS + MntMB + JFE), TPS + montmorillonite modified with dimethyl dihydrogenated tallow ammonium (TPS + MntMD), and TPS + montmorillonite modified with dimethyl dihydrogenated tallow ammonium containing Jamaica flower extract (TPS + MntMD + JFE)

orientation than the MntMB nano-filler, thus favoring the passage of water vapor (diffusion gradient) within the TPS matrix.

Opacity

As expected, the TPS film was the least opaque, i.e. the most transparent, of the films tested (Table 2), as by not containing nano-fillers within the carbohydrate polymer matrix that scatter light, this can pass through the material more easily. According to Gutiérrez and Alvarez (2018), more opaque food packaging materials can prevent or minimize damage caused by UV radiation to photosensitive substances such as pigments, vitamins, antioxidants, and polyunsaturated fatty acids contained in food. Thus, all the bionanocomposite films developed could be able to minimize photo-oxidative damage catalyzed by UV radiation on food, although the TPS + NMnt film (most opaque material) is the best adapted for this purpose. Interestingly, this was the material containing the least exfoliated and most interleaved nano-filler. In general, the bionanocomposite films containing the natural nano-fillers (TPS + NMnt and TPS + NMnt + JFE) showed the highest opacity values. Thus, it seems that the scarce exfoliation and high intercalation of these nano-fillers resulted in more opaque films. The film with the next highest opacity value was the TPS + MntMD + JFE film, which had the agglomerated nano-filler (MntMD + JFE) within the TPS matrix. Thus more interleaved, less exfoliated, and more agglomerated materials give more opaque bionanocomposite films.

Since the thickness values of the films analyzed were not significantly different ($p \geq 0.05$), variations in the opacity values could be positively associated with the chemical interactions that took place between the TPS matrix and the nano-fillers. According to Slavutsky et al. (2012), differences in opacity in nanocomposite thermoplastic materials obtained from starch-clay can be related to differences in the intercalation, exfoliation, and orientation of the nano-clays within the film matrices. Specifically, the parallel orientation of the nano-clays within the TPS matrix favors the passage of light, which results in less opaque (more transparent) materials (Slavutsky et al. 2012). The organo-clay nano-fillers (MntMB and MntMD) thus produced less opaque films than those containing the natural nano-filler without added JFE (TPS + NMnt), although statistically significant differences ($p \geq 0.05$) were not observed between the two film systems containing the two organo-modified nano-fillers without JFE (TPS + MntMB and TPS + MntMD). Thus, the organo-modification not only favors the exfoliation of the nano-fillers but also their orientation parallel to the direction of the thermo molding strength of the developed bionanocomposite films. It is worth noting that the direction of diffusion of the water vapor and the direction of the passage of light in the systems evaluated were also parallel to the force applied during film thermal molding. This means that the WVP values should be positively correlated with the opacity values. Some of the films containing the nano-fillers plus JFE (TPS + MntB + JFE and TPS + MntMD + JFE) were more opaque than their analogous films without JFE (TPS + MntB and TPS + MntMD). Thus apparently, the addition of JFE to the nano-fillers (pigment—anthocyanin) increases the opacity values. In contrast, the film containing the NMnt nano-filler without added JFE (TPS + NMnt) was more opaque than its analogue with added JFE (TPS + NMnt + JFE). Similar results were reported by Gutiérrez and Alvarez (2018) for bionanocomposite films prepared from corn starch and blueberry extract nanopackaged with clays.

Water Solubility (WS)

The water solubility (WS) values at 25 °C for the film systems analyzed are shown in Table 2. The solubility of bionanocomposite films gives an indication of their integrity in an aqueous medium, such that lower WS values indicate a higher water resistance, i.e. they are less water and moisture susceptible, which is a desired feature of food packaging

materials (Gutiérrez 2018). The TPS + MntMD film was the least water-soluble material. This film was also the one with the most exfoliated nano-filler (MntMD), the strongest nano-filler/starch interactions, and no phase separation. This confirms the positive effect of the exfoliated nano-fillers on the physicochemical properties of the bionanocomposite films. The TPS + MntMD film was, in fact, the only one to have a significantly lower ($p \leq 0.05$) WS than the TPS film, with the other bionanocomposite films either showing similar, or significantly higher WS values compared to the TPS film.

All the bionanocomposite films with added JFE within their layers were statistically ($p \leq 0.05$) more water soluble than their analogous bionanocomposite films without added JFE. In a previous study, Gutiérrez et al. (2018) demonstrated that the JFE (anthocyanins—polar compound) contained in the nano-clays migrates toward the aqueous medium. An increase in the WS of films containing nano-fillers with added JFE can thus be explained by phenomenon. The TPS + MntMB + JFE film proved to be the most water-soluble material. This may be explained by two factors: (1) the MntMB + JFE clay contained a higher molar fraction of JFE (0.10) within its layers than the MntMD + JFE clay (Gutiérrez et al. 2018), and (2) the MntMB + JFE clay was the more exfoliated JFE-containing nano-filler within the TPS matrix. This would increase the molar volume, thus facilitating the diffusion of the JFE toward the aqueous medium.

Scanning Electron Microscopy (SEM)

Figure 4 shows the SEM micrographs of the cryogenic fractured surfaces of the films studied. The morphologies of these surfaces were consistent with the results obtained from the XRD diffractograms (see Fig. 3, "X-ray diffraction" section), i.e. they were mainly amorphous starch-based films. It is worth noting that none of the films developed showed morphologies similar to starch granules, thus confirming the successful gelatinization and plasticization of these systems. This is important to note, since not all extrusion conditions guarantee the complete gelatinization and plasticization of the starch (Li et al. 2011).

The TPS film showed a smooth and compact morphology. In contrast, and as expected, the nano-fillers contained in the bionanocomposite films were observed within the structure of the TPS matrix. In particular, the TPS + NMnt and TPS + NMnt + JFE films showed low surface adhesion between the TPS matrix and the natural nano-fillers (NMnt and NMnt + JFE). These observations agree with the TGA results for these film systems where phase separation was also demonstrated. The lowest nano-filler/starch surface adhesion, however, was observed for the TPS + NMnt film. Thus the JFE nano-packed within the NMnt clay apparently improves TPS matrix/nano-filler compatibility. This is probably due not only to the greater degree of exfoliation of NMnt + JFE nano-filler compared to the NMnt nano-filler but also the possible plasticizing effect of the JFE within the TPS matrix. Recently, our research group observed similar behavior for pH-sensitive nano-fillers prepared from clay/blueberry extract within a TPS matrix (Gutiérrez and Alvarez 2018).

In general, the films containing the organo-modified nano-fillers showed greater surface adhesion between the TPS matrix and the nano-fillers than those containing natural nano-fillers (NMnt and NMnt + JFE). Granular particles were observed in the TPS + MntMB film, possibly associated with retrograded (recrystallized) starch, but not in the TPS + MntMB + JFE film. This would be in line with the higher crystallinity percentage observed for the former (6.37%) compared to the latter (5.24%) (see "X-ray diffraction" section 3.2), and shows that nanopackaging JFE within the clays has a beneficial effect by preventing starch retrogradation. The morphology of the TPS + MntMB + JFE film deserves special attention since, as can be observed, the particles of this nano-filler are oriented in a more parallel direction to each other within the TPS matrix than their analogue film (TPS + MntMB). This agrees with the higher WVP value obtained for the TPS + MntMB + JFE film compared to the TPS + MntMB film, and suggests that the microstructure of the former improves transport phenomena within the material.

As regards the TPS + MntMD and TPS + MntMD + JFE films, the former exhibited a compact microstructure with the nano-fillers mainly exfoliated without a preferential orientation, i.e. the nano-fillers were randomly dispersed within the matrix. In the TPS + MntMD + JFE film, however, as well as mainly exfoliated and randomly dispersed nano-filler particles, agglomerates of the nano-filler were also observed. This confirms that the MntMD + JFE nano-filler was partially exfoliated and agglomerated within the TPS matrix. Furthermore, it explains the higher crystallinity percentage of the TPS + MntMD + JFE film (7.50%) compared to its analogue film containing the same nano-filler but without added JFE (TPS + MntMD—4.84%).

Uniaxial Tensile Tests

The stress-strain curves of each film studied are shown in Fig. 5. A small linear zone followed by a nonlinear zone until breaking point was observed for all the systems. Similar behavior for corn starch-based films has been reported elsewhere in the literature (Ghanbarzadeh et al. 2011).

The majority of the scientific papers related to bionanocomposite films mainly focus on the mechanical behavior of these systems. However, the failure mechanisms and the fracture properties responsible for this behavior have been little studied (Bernal 2016). Pérez et al. (2013) suggested that there are two opposing failure mechanisms that can occur in TPS/nano-clay films: (1) a decoupling process caused by weak filler–matrix interactions, which leads to a subsequent

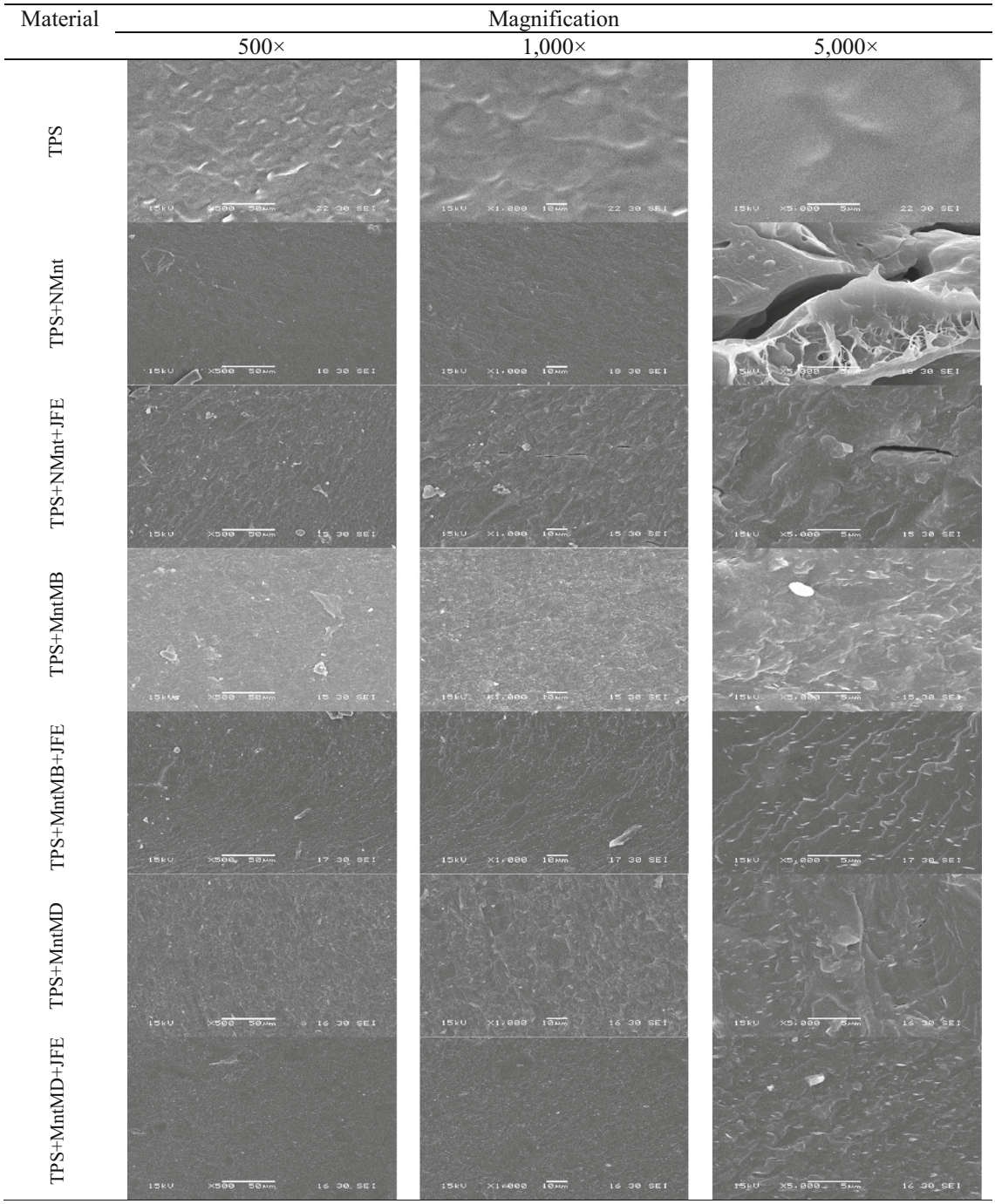

Fig. 4 SEM micrographs of the cryogenic fractured surface of the films based on: thermoplastic starch (TPS), TPS + natural montmorillonite (TPS + NMnt), TPS + natural montmorillonite containing Jamaica flower extract (TPS + NMnt + JFE), TPS + montmorillonite modified with dimethyl benzylhydrogenated tallow ammonium (TPS + MntMB), TPS + montmorillonite modified with dimethyl benzylhydrogenated tallow ammonium containing Jamaica flower extract (TPS + MntMB + JFE), TPS + montmorillonite modified with dimethyl dihydrogenated tallow ammonium (TPS + MntMD), and TPS + montmorillonite modified with dimethyl dihydrogenated tallow ammonium containing Jamaica flower extract (TPS + MntMD + JFE)

plastic deformation of the TPS matrix (increased toughness), and (2) the presence of agglomerates.

In order to carry out an exhaustive study of the mechanical behavior of the bionanocomposite films developed, the tests were carried out under quasi-static uniaxial tensile loading conditions at two different test speeds: 1 and 5 mm/s. Our first working hypothesis was that the nano-fillers subjected to the higher test speed would have less time to rearrange any orientation parallel to the uniaxial plane of deformation, resulting in mechanical behavior typical of a fragile material, i.e. higher

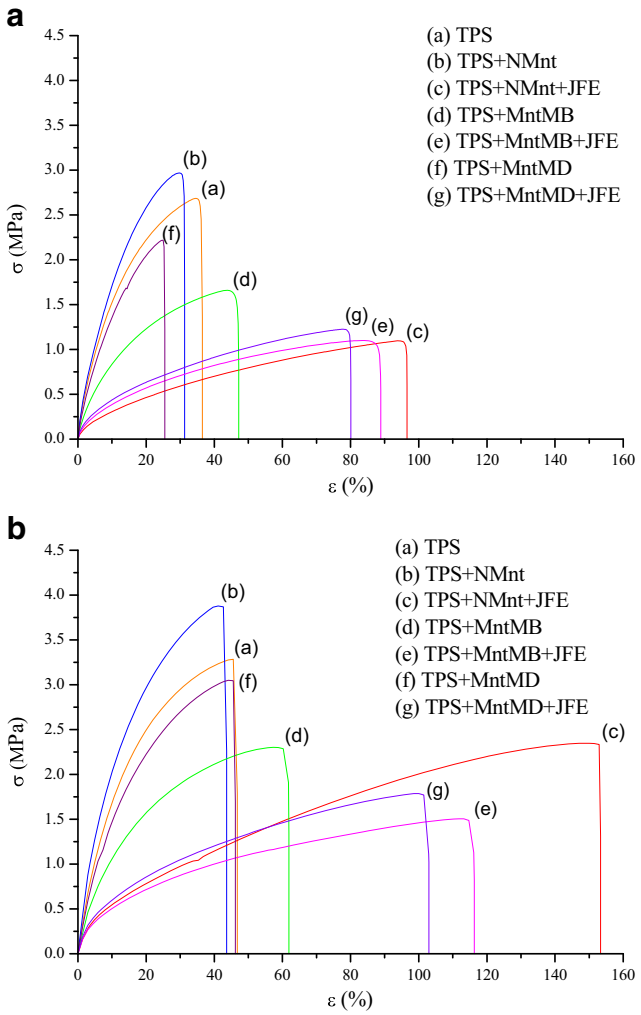

Fig. 5 **a** Stress (σ)-strain (ε) curves of the different films tested at 1 mm/s. **b** Stress (σ)-strain (ε) curves of the different films tested at 5 mm/s. Film systems: (a) thermoplastic starch (TPS), (b) TPS + natural montmorillonite (TPS + NMnt), (c) TPS + natural montmorillonite containing Jamaica flower extract (TPS + NMnt + JFE), (d) TPS + montmorillonite modified with dimethyl benzylhydrogenated tallow ammonium (TPS + MntMB), (e) TPS + montmorillonite modified with dimethyl benzylhydrogenated tallow ammonium containing Jamaica flower extract (TPS + MntMB + JFE), (f) TPS + montmorillonite modified with dimethyl dihydrogenated tallow ammonium (TPS + MntMD), and (g) TPS + montmorillonite modified with dimethyl dihydrogenated tallow ammonium containing Jamaica flower extract (TPS + MntMD + JFE)

Young's modulus (E) and maximum stress (σ_m) values should theoretically be obtained. As is well known, an increase in these values (E and σ_m) often leads to a loss in material plasticity (lower strain at break (ε_b) values) (Bernal 2016). In general, the results obtained (Fig. 6) show that the σ_m, ε_b, and toughness (T) values significantly increased ($p \leq 0.05$) when the bionanocomposite films were evaluated at a higher test speed (5 mm/s). Thus, following Pérez et al. (2013), the failure mechanism of these materials was due to weak nano-filler-TPS matrix interactions (hydrogen bonding interactions) leading to the plastic deformation of the TPS matrix (increased toughness). These results are in line with those obtained from the TGA analyses (see "Thermogravimetric analysis" section).

It is worth noting that in general, the mechanical behavior (trend) of the bionanocomposite films was similar at the two test speeds, thus suggesting that their analysis is independent of the test speed, while the considerations recommended by the standard (ISO 527-2 2012) are followed. Nevertheless, this study shows that not only the relative humidity in which the tests are carried out (Mali et al. 2005) and aging of the materials during storage (García-Tejeda et al. 2013) affects the mechanical properties of the films but also the test speed. This means that it would be incorrect to compare the mechanical properties between materials unless they are subjected to exactly the same processing and testing conditions.

Although the mechanical behavior (trend) of the bionanocomposite films was similar for the two test speeds, the E values were modified without a clear trend. Specifically, the TPS, TPS + NMnt, TPS + MntMB, and TPS + MntMD films had statistically lower E values ($p \leq 0.05$), while the TPS + NMnt + JFE and TPS + MntMB + JFE films had statistically higher E values ($p \leq 0.05$) when tested at a faster test speed (5 mm/s). This suggests that the JFE nanopackaged within the nano-clays activates the toughening mechanism of the bionanocomposite films. According to Cotterell et al. (2007), toughening mechanisms are activated by the presence of voids that initiate crazes; however, the structure or chemistry of nano-clays can inhibit multiple crazing of the polymer matrix. Pérez et al. (2013) observed that stronger nano-filler/matrix interactions prevent the formation of voids necessary to promote multiple cracking of the polymer matrix, which would lead to more brittle materials. We can thus conclude that the JFE nano-packed within the filosilicate layers of the nano-clays improves nano-filler/TPS matrix interactions, resulting in more rigid materials. This is consistent with the TGA results (see "Thermogravimetric analysis" section). In spite of this, the TPS + MntMD + JFE film did not show any statistically significant changes in the E values ($p \geq 0.05$) between the test speeds evaluated.

Frequently, clay nano-fillers have been used to reinforce the polymer matrix in order to increase the σ_m and E values (Bernal 2016). In this study, the only bionanocomposite film that fulfilled this task was the TPS + NMnt film, as it was the only one with σ_m and E values higher than the TPS film.

It has been established in the literature that bionanocomposite materials with nano-fillers that are oriented in a more parallel (longitudinal) manner to the direction of the uniaxial tensile assay will show higher σ_m and E values than nano-fillers that are oriented toward the other two directions mutually perpendicular to the uniaxial direction of the trial (Alvarez et al. 2006; Bernal 2016). The WVP results show that the nano-filler particles in the TPS + MntMB + JFE film

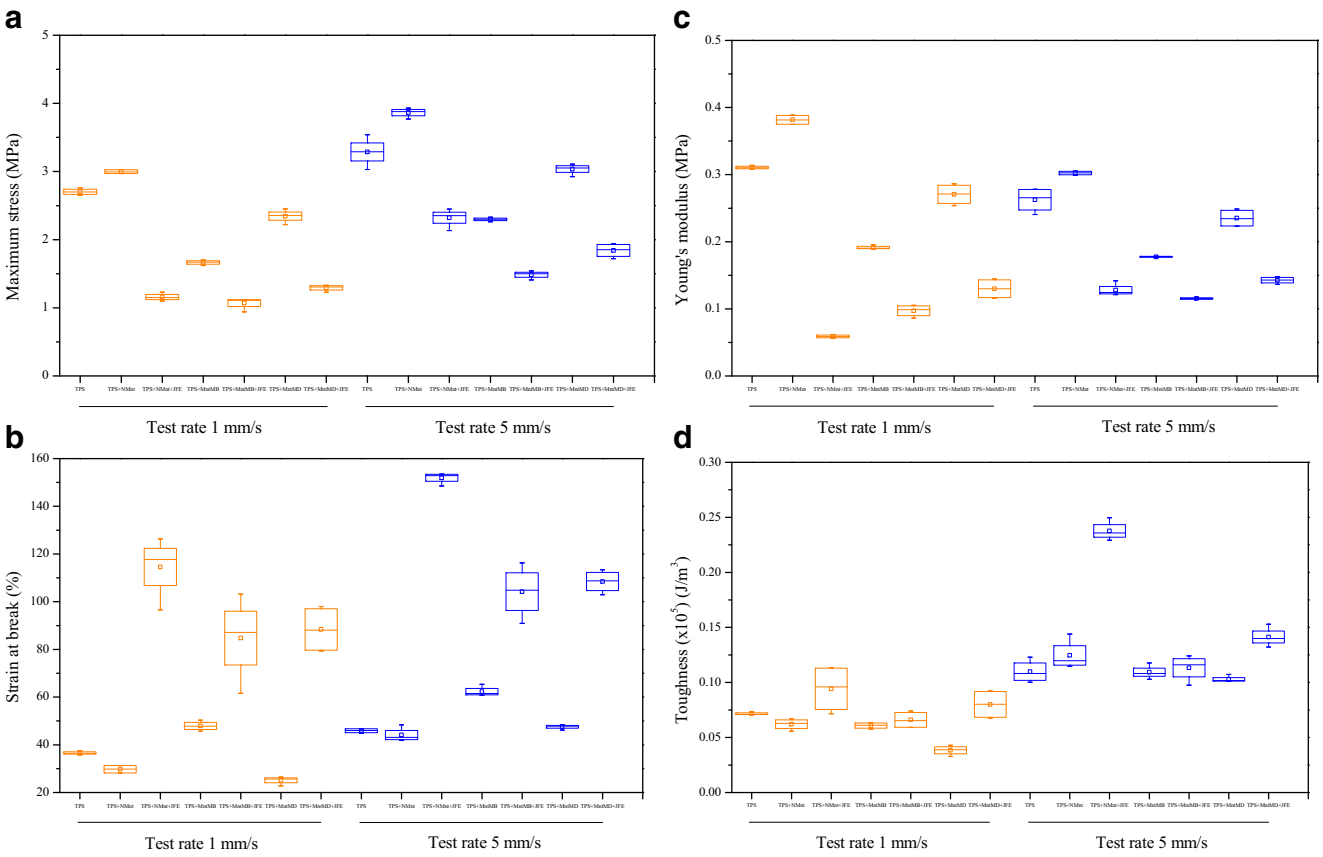

Fig. 6 Parameters of the uniaxial tensile strength tests: maximum stress (σ_m, **a**), strain at break (ε_b, **b**), Young's modulus (E, **c**), and toughness (T, **d**) of the different films tested at 1 and 5 mm/s. Film systems: thermoplastic starch (TPS), TPS + natural montmorillonite (TPS + NMnt), TPS + natural montmorillonite containing Jamaica flower extract (TPS + NMnt + JFE), TPS + montmorillonite modified with dimethyl benzylhydrogenated tallow ammonium (TPS + MntMB), TPS + montmorillonite modified with dimethyl benzylhydrogenated tallow ammonium containing Jamaica flower extract (TPS + MntMB + JFE), TPS + montmorillonite modified with dimethyl dihydrogenated tallow ammonium (TPS + MntMD), and TPS + montmorillonite modified with dimethyl dihydrogenated tallow ammonium containing Jamaica flower extract (TPS + MntMD + JFE)

were oriented parallel to each other. Nevertheless, the parallel orientation of these nano-fillers would be perpendicular to the direction of the uniaxial tensile test, i.e. transversally, since the results show that this was the film system with the lowest σ_m and E values. This occurs mainly because the propagation of the crack is longitudinal to the direction plane of the nano-fillers, where the nano-filler/matrix interaction energy is lowest (Bernal 2016). In addition, the nano-fillers act as barriers preventing the distribution of stresses along the matrix (Alvarez et al. 2006; Bernal 2016).

The σ_m and E values (Fig. 6a, c) were significantly lower ($p \leq 0.05$) in the films containing the fillers with the nanopackaged JFE compared to those containing the nano-fillers without JFE, as well as those containing the two organo-modified Mnt nano-fillers compared to those with the natural nano-filler. The incorporation of the Mnt modified with dimethyl benzylhydrogenated tallow ammonium lead to the greatest reduction in the σ_m and E values. In addition, a positive relationship between the σ_m and E values was observed, such that lower σ_m values correlated with lower E values.

All the bionanocomposite films containing the fillers with the nanopackaged JFE showed an increase in the ε_b values compared to the bionanocomposite films containing the nano-fillers without JFE (Fig. 6b). This may have been due to the plasticizing effect that anthocyanins (polyphenols) can generate within a TPS matrix. Similar results were reported by Gutiérrez and Alvarez (2018) for bionanocomposite films made from corn starch and nano-fillers containing anthocyanin extracts obtained from blueberries. The TPS + NMnt + JFE film was the most plastic material, followed by the TPS + MntMB + JFE and TPS + MntMD + JFE films. Although the difference between these last two film systems was not statistically significant ($p \geq 0.05$), the organo-modification of the Mnt with dimethyl benzylhydrogenated tallow ammonium did seem to somewhat improve the plastic behavior of the resulting film compared to the organo-modification with dimethyl dihydrogenated tallow ammonium.

The toughness values (Fig. 6d) were all similar among the films developed. Nevertheless, the bionanocomposite films with the JFE-containing nano-fillers did show slightly higher toughness values than the films containing the nano-fillers without JFE, probably due to the failure mechanism by toughening as described above. The TPS + NMnt + JFE film was the most tenacious material. According to Gutiérrez and Alvarez (2017c), films with higher toughness values can be especially useful to protect food during transport and storage, since these materials can absorb energy from knocks and bumps without this being transferred to the food.

Finally, the linear elastic fracture mechanics (LEFM) method could be used for a more in-depth study of the mechanical behavior of the film systems investigated here. This method is applicable to brittle materials that fail as a result of the growth of cracks after reaching a threshold load (Bernal 2016).

Antioxidant Activity—Response to pH Changes

Although the anthocyanin-containing nano-fillers were shown to have high antioxidant activity and be pH-sensitive (Gutiérrez et al. 2018), their incorporation into the TPS matrix did not confer either of these two properties on the resulting bionanocomposite films (Fig. 7). These results are similar to those previously reported by Gutiérrez and Alvarez (2018) for bionanocomposite film systems with added "active and intelligent" (A&I) nano-fillers obtained from natural and modified Mnt containing anthocyanins extracted from blueberries, although these were processed under slightly stronger extrusion conditions than those employed in this study. This is unfortunate since it suggests that the mass production of A&I films as food packaging materials using natural pigments could be seriously compromised under the conditions evaluated, since the films showed a poor performance as A&I films. Possibly, as these pigments are susceptible to degradation by the processes currently used in the polymer and food industries. Particularly, the high pressures generated inside the extruder limits its use. The measures that have been taken up to now to protect the pigment are also limited by several factors, such as (1) the extrusion temperature profile, (2) screw torque speed, and (3) the temperature and duration at which the thermo-molding of the material occurs. In addition, the development of pH-sensitive bionanocomposite films prepared from pH-sensitive nano-clays may be impeded by (1) the amount of nano-packed pigment within the nano-clay layers, and (2) the mechanism of pigment transport (migration and/or diffusion—diffusivity coefficient between the phases, mole fraction, and concentration gradient of the pigment) within

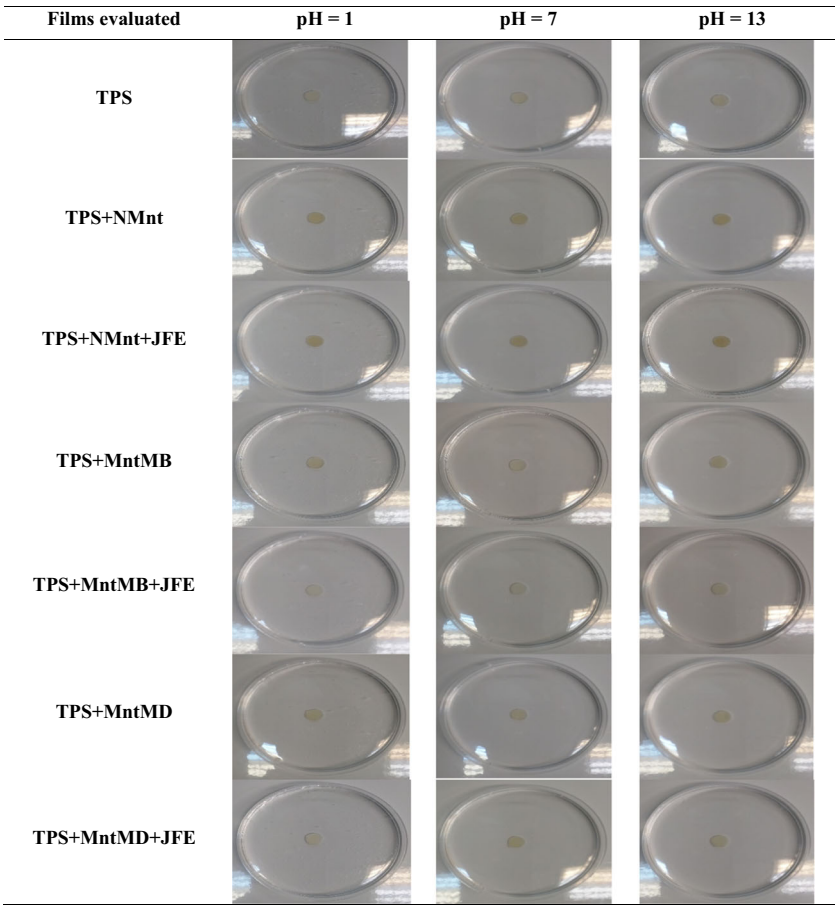

Fig. 7 Response of the different films studied at different pH conditions: thermoplastic starch (TPS), TPS + natural montmorillonite (TPS + NMnt), TPS + natural montmorillonite containing Jamaica flower extract (TPS + NMnt + JFE), TPS + montmorillonite modified with dimethyl benzylhydrogenated tallow ammonium (TPS + MntMB), TPS + montmorillonite modified with dimethyl benzylhydrogenated tallow ammonium containing Jamaica flower extract (TPS + MntMB + JFE), TPS + montmorillonite modified with dimethyl dihydrogenated tallow ammonium (TPS + MntMD), and TPS + montmorillonite modified with dimethyl dihydrogenated tallow ammonium containing Jamaica flower extract (TPS + MntMD + JFE)

the material from the nano-filler toward the surface of the thermoplastic material. A critical factor that we consider to be key to obtaining pH-sensitive films by extrusion is the high pressure generated inside the extruder, as a consequence of the shear forces generated by the screws. This hypothesis was based on the fact that the pigment has been shown to have a maximum thermal degradation temperature of around 211 °C (Gutiérrez et al. 2018), well above the conditions used for the processing of these materials. However, comparing this study with our previous one, we have observed that a decrease in screw torque speed does not achieve the complete exfoliation of the pH-sensitive nano-clays. This is undesirable, as it produces films with impaired mechanical properties. Finally, we can conclude that the use of pH-sensitive nano-clays as nano-fillers is complex, and there are still many factors that need to be studied before A&I bionanocomposite films can successfully be developed by extrusion.

Conclusions

The use of anthocyanins extracted from various plant sources has attracted the attention of food and polymer scientists and technologists due to the fact that they are natural pigments with active and pH-sensitive characteristics. The inclusion of anthocyanins as food additives in biopolymeric matrices could thus allow the development of "active and intelligent" (A&I) food packaging systems. The advantage of anthocyanins as nano-fillers, as compared to for example inorganic nanoparticles, is that the latter can represent a risk to health, and can also accumulate in different ecosystems, thus creating a potential toxic hazard. Furthermore, anthocyanins easily comply with the stringent international regulations that regulate the use of food additives. In this study, we aimed to develop active and pH-sensitive bionanocomposite films by extrusion. We were not able to achieve this, however, mainly due to the difficulty of obtaining complete starch gelatinization and complete exfoliation of the nano-clays, while keeping the pigment protected, when these materials are processed by extrusion. Despite this, we found that the mechanical properties and chemical interactions between the nano-fillers used were improved to the extent that the nano-clays were more exfoliated within the TPS matrix, thus preventing phase separation in the developed bionanocomposite films. Furthermore, the nano-packed anthocyanins obtained from the Jamaica (*Hibiscus sabdariffa*) flower extract had a positive effect on the compatibility of the materials developed, resulting in bionanocomposite films with improved mechanical and thermal properties. We also demonstrated that there are no absolute values of mechanical properties in starch-based films, even when the tests are performed under the same relative humidity and following the recommendations established by the standards, since the test speed also modifies these values. Nonetheless, it is worth noting that in general a similar trend in mechanical behavior between the samples was obtained at the two evaluated test speeds (1 and 5 mm/s) for the seven film systems analyzed.

Acknowledgements The authors would like to thank the Consejo Nacional de Investigaciones Científicas y Técnicas (CONICET) (Postdoctoral fellowship internal PDTS-Resolution 2417), Universidad Nacional de Mar del Plata (UNMdP) for financial support, and Dr. Mirian Carmona-Rodríguez for their valuable contribution. Many thanks also to Andres Torres Nicolini for all the assistance he provided in this research.

Data availability Transparency data associated with this article can be found in the online version at doi: 10.17632/382znrbc7f.1.

Compliance with Ethical Standards

Conflict of Interest The authors declare that they have no conflict of interest.

References

Abreu, A. S., Oliveira, M., de Sá, A., Rodrigues, R. M., Cerqueira, M. A., Vicente, A. A., & Machado, A. V. (2015). Antimicrobial nanostructured starch based films for packaging. *Carbohydrate Polymers, 129*, 127–134. https://doi.org/10.1016/j.carbpol.2015.04.021.

Altan, A., McCarthy, K. L., & Maskan, M. (2009). Effect of extrusion process on antioxidant activity, total phenolics and β-glucan content of extrudates developed from barley-fruit and vegetable by-products. *International Journal of Food Science & Technology, 44*(6), 1263–1271. https://doi.org/10.1111/j.1365-2621.2009.01956.x.

Alvarez, V., Vazquez, A., & Bernal, C. (2006). Effect of microstructure on the tensile and fracture properties of sisal fiber/starch-based composites. *Journal of Composite Materials, 40*(1), 21–35. https://doi.org/10.1177/0021998305053508.

Álvarez, K., Famá, L., & Gutiérrez, T. J. (2017). Physicochemical, antimicrobial and mechanical properties of thermoplastic materials based on biopolymers with application in the food industry. In M. Masuelli & D. Renard (Eds.), *Advances in Physicochemical Properties of Biopolymers: Part 1* (pp. 358–400). Bentham Science Publishers. https://doi.org/10.2174/9781681084534117010015.

ASTM E96-00e1. (2000). Standard test methods for water vapor transmission of materials. *ASTM International, West Conshohocken.* https://doi.org/10.1520/E0096-00E01.

Bernal, C. R. (2016). Fracture and failure of starch-based composites. In P. M. V. & L. Yu (Eds.), *Starch-based Blends, composites and nanocomposites* (pp. 326–351). Royal Society of Chemistry. https://doi.org/10.1039/9781782622796-00326.

von Borries-Medrano, E., Jaime-Fonseca, M. R., & Aguilar-Méndez, M. A. (2016). Starch-guar gum extrudates: Microstructure, physicochemical properties and in-vitro digestion. *Food Chemistry, 194*, 891–899. https://doi.org/10.1016/j.foodchem.2015.08.085.

Cazón, P., Velazquez, G., Ramírez, J. A., & Vázquez, M. (2017). Polysaccharide-based films and coatings for food packaging: a review. *Food Hydrocolloids, 68*, 136–148. https://doi.org/10.1016/j.foodhyd.2016.09.009.

Chevalier, E., Assezat, G., Prochazka, F., & Oulahal, N. (2018). Development and characterization of a novel edible extruded sheet based on different casein sources and influence of the glycerol

concentration. *Food Hydrocolloids, 75*, 182–191. https://doi.org/10.1016/j.foodhyd.2017.08.028.

Choi, I., Lee, J. Y., Lacroix, M., & Han, J. (2017). Intelligent pH indicator film composed of agar/potato starch and anthocyanin extracts from purple sweet potato. *Food Chemistry, 218*, 122–128. https://doi.org/10.1016/j.foodchem.2016.09.050.

Choudalakis, G., & Gotsis, A. D. (2009). Permeability of polymer/clay nanocomposites: A review. *European Polymer Journal, 45*(4), 967–984. https://doi.org/10.1016/j.eurpolymj.2009.01.027.

Cotterell, B., Chia, J. Y. H., & Hbaieb, K. (2007). Fracture mechanisms and fracture toughness in semicrystalline polymer nanocomposites. *Engineering Fracture Mechanics, 74*(7), 1054–1078. https://doi.org/10.1016/j.engfracmech.2006.12.023.

FAO. Food and Agriculture Organization of the United Nations. (2012). Pérdidas y desperdicio de alimentos en el mundo-Alcance, causas y prevención. Retrieved from http://www.fao.org/docrep/016/i2697s/i2697s.pdf

García-Tejeda, Y. V., López-González, C., Pérez-Orozco, J. P., Rendón-Villalobos, R., Jiménez-Pérez, A., Flores-Huicochea, E., Solorza-Feria, J., & Bastida, C. A. (2013). Physicochemical and mechanical properties of extruded laminates from native and oxidized banana starch during storage. *LWT - Food Science and Technology, 54*(2), 447–455. https://doi.org/10.1016/j.lwt.2013.05.041.

Ghanbarzadeh, B., Almasi, H., & Entezami, A. A. (2011). Improving the barrier and mechanical properties of corn starch-based edible films: effect of citric acid and carboxymethyl cellulose. *Industrial Crops and Products, 33*(1), 229–235. https://doi.org/10.1016/j.indcrop.2010.10.016.

Gutiérrez, T. J. (2017). Effects of exposure to pulsed light on molecular aspects of edible films made from cassava and taro starch. *Innovative Food Science & Emerging Technologies, 41*, 387–396. https://doi.org/10.1016/j.ifset.2017.04.014.

Gutiérrez, T. J. (2018). Active and intelligent films made from starchy sources/blackberry pulp. *Journal of Polymers and the Environment, 26*(6), 2374–2391. https://doi.org/10.1007/s10924-017-1134-y.

Gutiérrez, T. J., & Álvarez, K. (2017). Transport phenomena in biodegradable and edible films. In M. A. Masuelli (Ed.), *Biopackaging* (pp. 59–89). CRC Press Taylor & Francis Group Retrieved from https://www.crcpress.com/Biopackaging/Masuelli/p/book/9781498749688.

Gutiérrez, T. J., & Alvarez, V. A. (2017a). Cellulosic materials as natural fillers in starch-containing matrix-based films: a review. *Polymer Bulletin, 74*(6), 2401–2430. https://doi.org/10.1007/s00289-016-1814-0.

Gutiérrez, T. J., & Alvarez, V. A. (2017b). Eco-friendly films prepared from plantain flour/PCL blends under reactive extrusion conditions using zirconium octanoate as a catalyst. *Carbohydrate Polymers, 178*, 260–269. https://doi.org/10.1016/j.carbpol.2017.09.026.

Gutiérrez, T. J., & Alvarez, V. A. (2017c). Properties of native and oxidized corn starch/polystyrene blends under conditions of reactive extrusion using zinc octanoate as a catalyst. *Reactive and Functional Polymers, 112*, 33–44. https://doi.org/10.1016/j.reactfunctpolym.2017.01.002.

Gutiérrez, T. J., & Alvarez, V. A. (2018). Bionanocomposite films developed from corn starch and natural and modified nano-clays with or without added blueberry extract. *Food Hydrocolloids, 77*, 407–420. https://doi.org/10.1016/j.foodhyd.2017.10.017.

Gutiérrez, T. J., Tapia, M. S., Pérez, E., & Famá, L. (2015). Edible films based on native and phosphated 80:20 waxy: normal corn starch. *Starch - Stärke, 67*(1–2), 90–97. https://doi.org/10.1002/star.201400164.

Gutiérrez, T. J., Ponce, A. G., & Alvarez, V. A. (2017). Nano-clays from natural and modified montmorillonite with and without added blueberry extract for active and intelligent food nanopackaging materials. *Materials Chemistry and Physics, 194*, 283–292. https://doi.org/10.1016/j.matchemphys.2017.03.052.

Gutiérrez, T. J., León, I. E., Ponce, A. G., & Alvarez, V. A. (2018). Stabilizing effect of montmorillonite on anthocyanins extracted from Jamaica (*Hibiscus sabdariffa*) flowers: characterization and assessment of cytotoxicity. *Food Packaging and Shelf Life.* In press.

Han, J. H., & Floros, J. D. (1997). Casting antimicrobial packaging films and measuring their physical properties and antimicrobial activity. *Journal of Plastic Film & Sheeting, 13*(4), 287–298. https://doi.org/10.1177/875608799701300405.

Iman, M., & Maji, T. K. (2012). Effect of crosslinker and nanoclay on starch and jute fabric based green nanocomposites. *Carbohydrate Polymers, 89*(1), 290–297. https://doi.org/10.1016/j.carbpol.2012.03.012.

ISO 527-2. (2012). Determination of tensile properties of plastics. Retrieved from https://www.iso.org/obp/ui/#iso:std:56046:en

Li, M., Liu, P., Zou, W., Yu, L., Xie, F., Pu, H., Liu, H., & Chen, L. (2011). Extrusion processing and characterization of edible starch films with different amylose contents. *Journal of Food Engineering, 106*(1), 95–101. https://doi.org/10.1016/j.jfoodeng.2011.04.021.

Liu, B., Xu, H., Zhao, H., Liu, W., Zhao, L., & Li, Y. (2017). Preparation and characterization of intelligent starch/PVA films for simultaneous colorimetric indication and antimicrobial activity for food packaging applications. *Carbohydrate Polymers, 157*, 842–849. https://doi.org/10.1016/j.carbpol.2016.10.067.

Luchese, C. L., Frick, J. M., Patzer, V. L., Spada, J. C., & Tessaro, I. C. (2015). Synthesis and characterization of biofilms using native and modified pinhão starch. *Food Hydrocolloids, 45*, 203–210. https://doi.org/10.1016/j.foodhyd.2014.11.015.

Luchese, C. L., Garrido, T., Spada, J. C., Tessaro, I. C., & de la Caba, K. (2018). Development and characterization of cassava starch films incorporated with blueberry pomace. *International Journal of Biological Macromolecules, 106*, 834–839. https://doi.org/10.1016/j.ijbiomac.2017.08.083.

Ludueña, L., Morán, J., & Alvarez, V. (2015). Biodegradable polymer/clay nanocomposites. In V. K. Thakur & M. K. Thakur (Eds.), *Eco-friendly polymer nanocomposites: processing and properties* (pp. 109–135). New Delhi: Springer India. https://doi.org/10.1007/978-81-322-2470-9_4.

Ma, Q., & Wang, L. (2016). Preparation of a visual pH-sensing film based on tara gum incorporating cellulose and extracts from grape skins. *Sensors and Actuators B: Chemical, 235*, 401–407. https://doi.org/10.1016/j.snb.2016.05.107.

Mali, S., Sakanaka, L. S., Yamashita, F., & Grossmann, M. V. E. (2005). Water sorption and mechanical properties of cassava starch films and their relation to plasticizing effect. *Carbohydrate Polymers, 60*(3), 283–289. https://doi.org/10.1016/j.carbpol.2005.01.003.

Miller, N. J., & Rice-Evans, C. A. (1997). Factors influencing the antioxidant activity determined by the ABTS•+ radical cation assay. *Free Radical Research, 26*(3), 195–199. https://doi.org/10.3109/10715769709097799.

Moreno, O., Cárdenas, J., Atarés, L., & Chiralt, A. (2017). Influence of starch oxidation on the functionality of starch-gelatin based active films. *Carbohydrate Polymers, 178*, 147–158. https://doi.org/10.1016/j.carbpol.2017.08.128.

Müller, C. M. O., Laurindo, J. B., & Yamashita, F. (2011). Effect of nanoclay incorporation method on mechanical and water vapor barrier properties of starch-based films. *Industrial Crops and Products, 33*(3), 605–610. https://doi.org/10.1016/j.indcrop.2010.12.021.

Pereira, V. A., de Arruda, I. N. Q., & Stefani, R. (2015). Active chitosan/PVA films with anthocyanins from Brassica oleraceae (red cabbage) as time–temperature indicators for application in intelligent food packaging. *Food Hydrocolloids, 43*, 180–188. https://doi.org/10.1016/j.foodhyd.2014.05.014.

Pérez, E., Pérez, C. J., Alvarez, V. A., & Bernal, C. (2013). Fracture behavior of a commercial starch/polycaprolactone blend reinforced with different layered silicates. *Carbohydrate Polymers, 97*(2), 269–276. https://doi.org/10.1016/j.carbpol.2013.04.099.

Rhim, J.-W., & Kim, Y.-T. (2014). Biopolymer-based composite packaging materials with nanoparticles. In S. L. Taylor (Ed.), *Innovations in Food Packaging* (second ed., pp. 413–442). Amsterdam: Elsevier. https://doi.org/10.1016/B978-0-12-394601-0.00017-5.

Rincón, M., Tapia, M. S., & Padilla, F. (2003). Evaluación de fitoquímicos en el exocarpio (cáscara) de algunas frutas cultivadas en Venezuela. *Revista Facultad de Farmacia, 66*(2), 73–78.

Risch, S. J. (2009). Food packaging history and innovations. *Journal of Agricultural and Food Chemistry, 57*(18), 8089–8092. https://doi.org/10.1021/jf900040r.

Romero-Bastida, C. A., Tapia-Blácido, D. R., Méndez-Montealvo, G., Bello-Pérez, L. A., Velázquez, G., & Alvarez-Ramirez, J. (2016). Effect of amylose content and nanoclay incorporation order in physicochemical properties of starch/montmorillonite composites. *Carbohydrate Polymers, 152*, 351–360. https://doi.org/10.1016/j.carbpol.2016.07.009.

Slavutsky, A. M., Bertuzzi, M. A., & Armada, M. (2012). Water barrier properties of starch-clay nanocomposite films. *Brazilian Journal of Food Technology, 15*(3), 208–218 Retrieved from http://www.scielo.br/scielo.php?script=sci_arttext&pid=S1981-67232012000300004&nrm=iso.

Vasanthan, T., & Hoover, R. (1992). Effect of defatting on starch structure and physicochemical properties. *Food Chemistry, 45*(5), 337–347. https://doi.org/10.1016/0308-8146(92)90034-Y.

Vazquez, A., Cyras, V. P., Alvarez, V. A., & Moran, J. I. (2012). Starch/clay nano-biocomposites. In L. Avérous & E. Pollet (Eds.), *Environmental Silicate Nano-Biocomposites* (pp. 287–321). London: Springer London. https://doi.org/10.1007/978-1-4471-4108-2_11.

Wilpiszewska, K., Antosik, A. K., & Spychaj, T. (2015). Novel hydrophilic carboxymethyl starch/montmorillonite nanocomposite films. *Carbohydrate Polymers, 128*, 82–89. https://doi.org/10.1016/j.carbpol.2015.04.023.

Xie, D. F., Martino, V. P., Sangwan, P., Way, C., Cash, G. A., Pollet, E., Dean, K. M., Halley, P. J., & Avérous, L. (2013). Elaboration and properties of plasticised chitosan-based exfoliated nanobiocomposites. *Polymer, 54*(14), 3654–3662. https://doi.org/10.1016/j.polymer.2013.05.017.

Xie, M., Duan, Y., Li, F., Wang, X., Cui, X., Bacha, U., Zhu, M. P., Xiao, Z., & Zhao, Z. (2017). Preparation and characterization of modified and functional starch (hexadecyl corboxymethyl starch) ether using reactive extrusion. *Starch - Stärke, 69*(5–6), 1600061. https://doi.org/10.1002/star.201600061.

Yoshida, C. M. P., Maciel, V. B. V., Mendonça, M. E. D., & Franco, T. T. (2014). Chitosan biobased and intelligent films: monitoring pH variations. *LWT - Food Science and Technology, 55*(1), 83–89. https://doi.org/10.1016/j.lwt.2013.09.015.

Zeppa, C., Gouanvé, F., & Espuche, E. (2009). Effect of a plasticizer on the structure of biodegradable starch/clay nanocomposites: thermal, water-sorption, and oxygen-barrier properties. *Journal of Applied Polymer Science, 112*(4), 2044–2056. https://doi.org/10.1002/app.29588.